ELSEVIER

NeuroImage

www.elsevier.com/locate/ynimg
NeuroImage 31 (2006) 993 – 1003

Mapping anatomical correlations across cerebral cortex (MACACC) using cortical thickness from MRI

Jason P. Lerch,[a] Keith Worsley,[a] W. Philip Shaw,[b] Deanna K. Greenstein,[b] Rhoshel K. Lenroot,[b] Jay Giedd,[b] and Alan C. Evans[a,*]

[a]*McConnell Brain Imaging Centre, Montreal Neurological Institute, McGill University, 3801 University Street, Montreal, QC, Canada H3A 2B4*
[b]*National Institute of Mental Health, National Institutes of Health, Department of Health and Human Services, Bethesda, MD, USA*

Received 3 June 2005; revised 22 December 2005; accepted 12 January 2006
Available online 19 April 2006

We introduce MACACC-Mapping Anatomical Correlations Across Cerebral Cortex-to study correlated changes within and across different cortical networks. The principal topic of investigation is whether the thickness of one area of the cortex changes in a statistically correlated fashion with changes in thickness of other cortical regions. We further extend these methods by introducing techniques to test whether different population groupings exhibit significantly varying MACACC patterns. The methods are described in detail and applied to a normal childhood development population (n = 292), and show that association cortices have the highest correlation strengths. Taking Brodmann Area (BA) 44 as a seed region revealed MACACC patterns strikingly similar to tractography maps obtained from diffusion tensor imaging. Furthermore, the MACACC map of BA 44 changed with age, older subjects featuring tighter correlations with BA 44 in the anterior portions of the superior temporal gyri. Lastly, IQ-dependent MACACC differences were investigated, revealing steeper correlations between BA 44 and multiple frontal and parietal regions for the higher IQ group, most significantly (t = 4.0) in the anterior cingulate.
© 2006 Published by Elsevier Inc.

Introduction

The cerebral cortex is organized into networks of functionally complementary areas. Classic examples include the dorsal and ventral visual streams, the limbic system, and the language networks. These networks are traditionally studied using functional paradigms designed to reveal the particular role of a certain area. Examples of such studies include the role of Broca's Area in word repetition, synonym generation (Klein et al., 1997), verbal fluency (Frith et al., 1991), speech production (Buckner et al., 1995) and silent word production (Friedman et al., 1998).

Functional specialization can also lead to related anatomical change. A recent study investigated the size of the hippocampus, a structure involved in spatial navigation, in London taxi drivers and found increases in size correlating with increased experience in navigating the streets of London (Maguire et al., 2000, 2003). Similarly, faster phonetic learners were found to have greater white matter density in parietal regions than slower learners (Golestani et al., 2002). Trained musicians feature enlarged primary motor and sensorimotor areas, premotor areas, anterior superior parietal areas, and inferior temporal gyri (Schlaug, 2001; Gaser and Schlaug, 2003a,b). This last example involving musicians is particularly informative as it involves multiple cortical areas, including motor, sensorimotor, and multimodal sensory areas, collaborating. Increases in anterior corpus callosum size further suggests that the intra-hemispheric connectivity of the brain is enhanced in trained musicians (Schlaug, 2001).

We propose to address a related but less explored topic: as the anatomy of one cortical area changes, are there correlated morphological changes in other cortical areas? An example hypothesis from the language-processing domain might be that a population with thicker cortices in Broca's Area will have a correspondingly larger Wernicke's Area.

The connectivity of the human cerebral cortex is not a new topic of investigation. It has traditionally been studied using fiber tracing, wherein a seed region is injected with a retrograde tracer in order to determine which areas have direct fibre connections to the seed region (Romanski et al., 1999; Petrides and Pandya, 2002). More recently the notion of functional connectivity has been promoted, i.e. areas that are functionally related will feature correlated change in a fMRI or PET functional activation study (Friston, 2002; Friston et al., 1993, 1996, 2003; Koski and Paus, 2000; Horwitz, 2003; Lee et al., 2003; Ramnani et al., 2004).

We propose to study correlated anatomical changes using methods related to functional connectivity but employing morphometric data; we have dubbed this approach Mapping Anatomical Correlation Across Cerebral Cortex (MACACC). Of particular interest will be not just testing which areas of the cortex correlate with which other areas, but also whether the MACACC patterns vary across different categorical groupings based on demographical variables (age, gender, socio-economic status) or clinical diagnoses.

* Corresponding author. Fax: +1 514 398 8952.
E-mail address: alan@bic.mni.mcgill.ca (A.C. Evans).
Available online on ScienceDirect (www.sciencedirect.com).

1053-8119/$ - see front matter © 2006 Published by Elsevier Inc.
doi:10.1016/j.neuroimage.2006.01.042

The methods used in MACACC involve statistical analyses of data extracted from anatomical MRI using the metric of cortical thickness, which features several advantageous properties for MACACC:

1. It covers the entire cortex.
2. It provides a biologically meaningful measurement (cortical thickness).
3. It has a reduced number of points compared to volumetric data (40,962 vertices versus 1,000,000 voxels).

The methods developed herein should, however, also be applicable to other anatomical data such as, for example, voxel density measures from Voxel Based Morphometry (VBM) (Ashburner and Friston, 2000; Watkins et al., 2001). Some statistical issues have been explored in (Worsley et al., 2005).

We use this technique to address two core developmental issues. Firstly, several strands of evidence suggest that anatomical and functional interconnections between Broca's and Wernicke's areas may increase with age (Paus et al., 1999). Language becomes more lateralized (Holland et al., 2001) and DTI studies of the white matter tract connecting Broca's and Wernickes' areas shows changes in indirect measures of integrity (fractional anisotropy) (Schmithorst et al., 2002). Moreover, in an adult population, functional imaging studies demonstrate increased activity of Brodmann Area 44 (BA 44) during language processing (Amunts et al., 2004). We thus predict that the correlation in cortical thickness of these two language processing regions would show a developmental gradient, increasing with age. Secondly, intelligence is linked to brain activity. Greater brain activity during intellectually demanding activity has been shown using fMRI in individuals of greater general intelligence in an extensive network comprising lateral frontal and parietal regions (Gray et al., 2003). Others report similar alterations in functional connectivity linked to intelligence (Haier et al., 2004) which may be underpinned by enhanced structural connectivity. We hypothesize that, as seen in the motor learning examples given above, the functional enhancements are mirrored by concomitant change in the underlying neural substrate which can be detected by MRI-based morphometry, e.g. MACACC. The population used herein comes from a study of normal childhood brain development (Giedd, 2004; Gogtay et al., 2004). The purpose is not to provide a definitive account of these latter two questions but rather to illustrate the concept of MACACC, leaving more detailed study of brain development for future work.

Methods

The methods used to study MACACC can be subdivided into: (1) the extraction of the morphometric data and, (2) the statistical techniques used to ascertain the correlations. A summary of all the definitions used throughout is included in Table 1.

Extraction of morphometric data

The input metric for MACACC studies is cortical thickness as measured from MRI. The choice of MR sequence is immaterial as long as sufficient resolution and grey/white matter contrast are provided and subject groups to be compared were not acquired using different sequences. The native MR image is corrected for non-uniformity artefacts (Sled et al., 1998) and registered into stereotaxic space using a nine parameter linear transformation (Collins et al., 1994). Cerebral tissue is classified into white matter, gray matter, spinal fluid and background using a neural net classifier (Zijdenbos et al., 2002). The inner and outer cortical surfaces are then extracted using deformable surface-mesh models (MacDonald et al., 2000; Kim et al., 2005) and non-linearly aligned towards a standard template surface (Robbins et al., 2004). Cortical thickness is measured in native-space millimetres using the linked distance between the white and pial surfaces, tlink (MacDonald et al., 2000; Lerch and Evans, 2005). The thickness map is blurred using a 30 mm surface based diffusion smoothing kernel (Chung et al., 2003). These methods have been validated using both manual measurements (Kabani et al., 2001) and a population simulation (Lerch and Evans, 2005), and used in an Alzheimer's Disease population study (Lerch et al., 2005). Closely related methods have also been applied to Huntington's (Rosas et al., 2002) and normal ageing (Salat et al., 2004) among others. Example output can be seen in Fig. 1.

Table 1
Definition of terms: a list of the definitions used throughout the paper

Name	Definition
Correlation	Measured using Pearson's *r*, relates to the strength of the correlation between a seed region and the rest of the cortex.
MACACC-strength	The average correlation coefficient when every vertex is correlated with every other vertex.
MACACC-slope	Shows a group difference in the estimated slope between the seed region and target vertex.
MACACC-variance	Shows a group difference in the variance around the estimated slope between the seed region and target vertex.

Statistical techniques

Measuring MACACC can be subdivided into two main components: assessing cross-cortical correlations as well as quantifying differences in MACACC maps across groups.

MACACC methods—correlations

Cortical cross-correlations are obtained using simple linear correlations whose strength is measured using Pearson's *r*.

$$r = \frac{\sum T_i T_j - \frac{\sum T_i \sum T_j}{N_s}}{\sqrt{\left(\sum T_i^2 - \frac{\left(\sum T_i\right)^2}{N_s}\right)\left(\sum T_j^2 - \frac{\left(\sum T_j\right)^2}{N_s}\right)}} \quad (1)$$

Eq. (1) Pearson's *r*. Where T_i and T_j represent cortical thickness at the two vertices to be correlated with each other and *N*s is the total number of subjects. Summations are performed over *N*s.

Pearson's *r* takes on a value between 1 and −1, the sign referring to whether the correlation is positive or negative, and the closer to 1 or −1 the more significant the correlation. Equivalently, though slower computationally, is the use of a linear model wherein the seed region T_i (the area whose MACACC one is

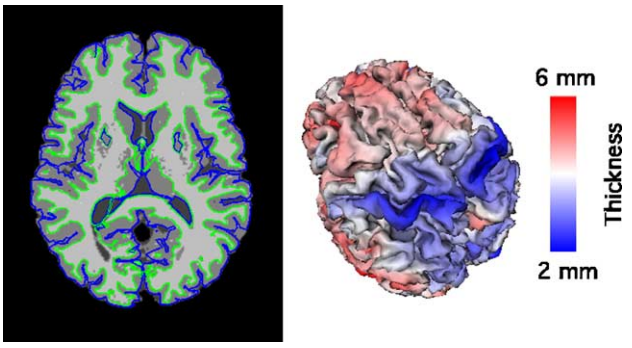

Fig. 1. Example of cortical thickness map, showing (on the left) the intersection of the pial surface (blue) and the white matter surface (green) on a transverse slice of the tissue classification map. On the right is a cortical surface colour coded with cortical thickness.

measuring) is modelled by target region T_j (independently at every vertex of the rest of the cortex).

$$T_i = \beta_0 + \beta_1 T_j + \varepsilon. \quad (2)$$

Eq. (2) Linear Model. Where the thickness of seed region T_i is modelled by a linear model of thickness of T_j plus a normally distributed error ε, estimated through an intercept term β_0 and slope β_1.

The significance of the linear model is measured using the Student's t statistics with N-1 degrees of freedom.

If a hypothesis exists, then one can target a seed region or vertex and explore its cortical cross-correlations. In the absence of a hypothesis a less directed search is needed. We therefore introduce the concept of MACACC-strength which measures the mean r value for the correlation against all other vertices at each vertex.

$$\mathrm{MACACCs}_i = \frac{\sum_{j=1}^{N_v}\left(\frac{\sum T_i T_j - \frac{\sum T_i \sum T_j}{N_s}}{\sqrt{\left(\sum T_i^2 - \frac{\left(\sum T_i\right)^2}{N_s}\right)\left(\sum T_j^2 - \frac{\left(\sum T_j\right)^2}{N_s}\right)}}\right)}{N_v} = \frac{\sum_{j=1}^{N_v} r}{N_v}. \quad (3)$$

Eq. (3) MACACC-strength: where $\mathrm{MACACCs}_i$ is the MACCACC strength at seed point i, N_v is the number of vertices, N_s is the number of subjects, T_i is the thickness at seed point i, and T_j is the thickness at target point j.

MACACC-strength is an $N_v \times N_v$ process and therefore computationally expensive. The current surface extraction procedure results in 40,962 vertices, a total of 40962 × 40962 correlations are needed. The true measure of MACACC-strength can be approximated, however, by correlating the thickness at every vertex against each subject's mean cortical thickness averaged over all 40,962 vertices. The results will be identical if the standard deviation is exactly the same at every node, which is known to not be the case (Lerch and Evans, 2005). The approximation is, however, a lot quicker to compute and should give a good indication of the true MACACC-strength result.

Assessing group differences

The second component of MACACC is testing for group differences. The question to be addressed is whether the MACACC maps between two or more groups are significantly different. For example, does the MACACC map for BA 44, which shows a significant correlation with the superior temporal gyrus, change across different age ranges? There are two different hypotheses that can be tested:

1. Differences in MACACC slope.
2. Differences in MACACC variance.

MACACC-slope. In the case of MACACC-slope the type of correlation between groups is different, i.e. it is steeper in one group than another (Fig. 2a), whereas in MACACC-variance the slope is potentially the same but the goodness of fit of the linear correlation is different (Fig. 2b).

Testing for the difference in slope is performed using a classic interaction linear model.

$$T_i = \beta_0 + \beta_1 T_j + \beta_2 \mathrm{Group} + \beta_3 \left(T_j{*}\mathrm{Group}\right) + \varepsilon. \quad (4)$$

Eq. (4) Interaction Model testing for differences in the relationship between T_i and T_j cortical thickness among the different factors present in Group. The Group component is modelled using treatment contrasts. The estimated terms are: β_0 is the intercept term, β_1 models the relationship between T_i and T_j, β_2 models the relationship between the group term and T_i, β_3 models the relationship between the interaction term (group by T_j) and T_i.

The factors in the Group variable (which could represent age groupings, for example) in the linear model described above are created using treatment contrasts, significance tested using Student's t statistic. One can also think of this problem with the following formulation: is the data better fit by a model that contains separate slopes for each group rather than a common slope?

MACACC-variance. One of the assumptions behind least-squares fits is that the error distribution along each dimension have equal variance, i.e. homoscedasticity. Given the example in Fig. 2b, this assumption will not necessarily hold in MACACC analyses. We therefore use a general least squares approach allowing unequal variances for each group in the classification factor (Pinheiro and Bates, 2000). Testing for differences in MACACC-variance is more complex than MACACC-slope, as the statistical methods are less well established. The criteria for a valid test are that it:

(1) Capture difference in variances across multiple groups.
(2) Has a defined model rejecting the assumption of equal variance H0.
(3) Be robust against outliers.

After the correlation slope has been determined, we must then test for whether the residuals by group are homoscedastic (have equal variance) or heteroscedastic (have unequal variance). Residuals are obtained by fitting a linear model relating T_i and T_j and subtracting the observed response from the predicted response.

Linear Model: $T_i = \beta_0 + \beta_1 T_j + \varepsilon$

Residual: $e_i = T_i - \beta_0 - \beta_1 T_j.$ (5)

Eq. (5) Linear model residuals.

Three tests were assessed in this study:

(1) F test for variance.
(2) Bartlett's test.
(3) Levene's test.

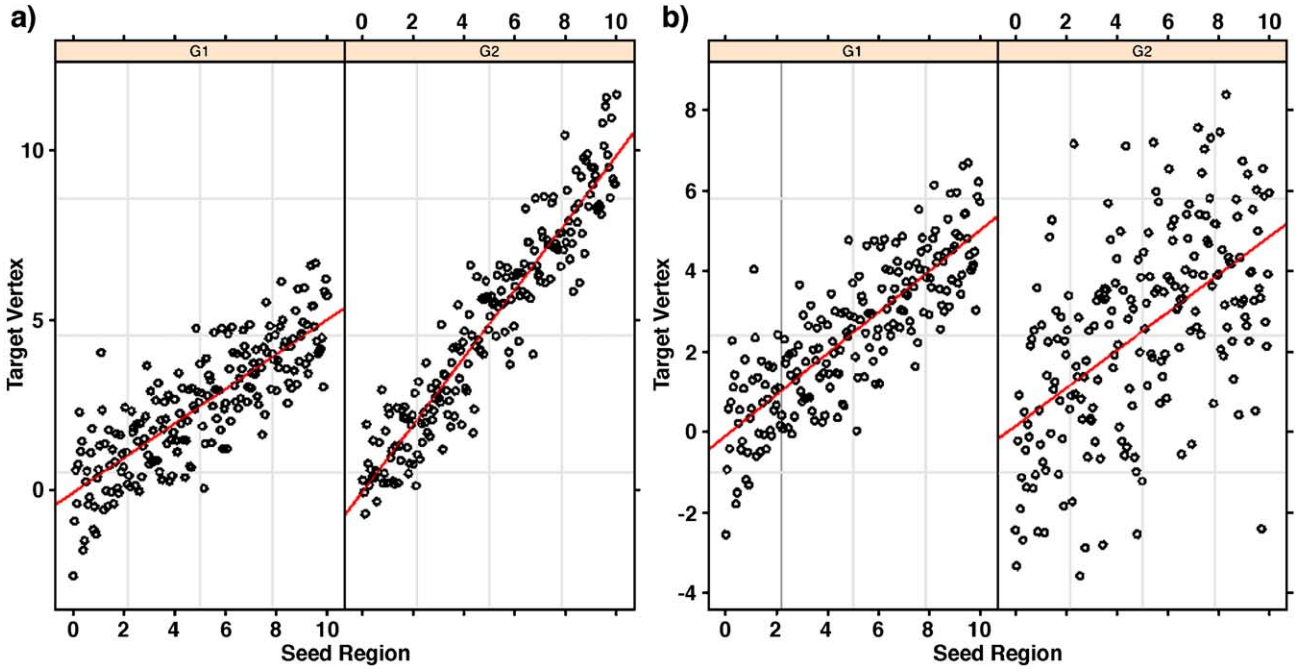

Fig. 2. Group differences: the two graphs above show the difference between MACACC-slope and MACACC-variance using simulated data. Graph a shows a correlation between target and seed regions where the variance between the two groups is the same, the slope different, being steeper in group G2. Graph b shows the same slope in the target vertex to seed region correlation, but the variance is higher in group G2 than G1. Graph a would thus be captured using MACACC-slope tests (interactions are significant at $P < 2.2 \times 10^{-16}$, variance not significant), graph b using MACACC-variance tests (interactions not significant, variance significant at $P < 3.9 \times 10^{-8}$).

The F test for variance is the simplest of the three, containing solely the ratio of two group variances.

$$s_1^2 = \frac{1}{N_1 - 1} \sum_{i=1}^{N_1} \left(G1_{e_i} - \hat{G1}_e \right)$$

$$s_2^2 = \frac{1}{N_2 - 1} \sum_{i=1}^{N_2} \left(G2_{e_i} - \hat{G2}_e \right)$$

$$F = \frac{s_1^2}{s_2^2}. \tag{6}$$

Eq. (6) F test for variance. G1 and G2 represent the two groups, N_1 and N_2 the respective group sizes, e_i the residuals as determined in Eq. (5).

The F test has two fundamental limitations: it is limited to two groups and is highly non-robust against outliers.

Bartlett's test and Levene's test are designed to overcome limitations of the F test. Bartlett's test measures the squared deviations from the group mean, Levene's the absolute deviation from the group mean, median, or trimmed mean (NIST/SEMATECH, 2005).

Eq. (7) Bartlett's Test, which results in a $\times^2$ distribution of k-1 degrees of freedom (NIST/SEMATECH, 2005).

$$T = \frac{(N-k)\ln s_P^2 - \sum_{i=1}^{k} (N_i - 1)\ln s_i^2}{1 + \left(1/3\left(k-1\right)\right)\left(\left(\sum_{i=1}^{k} 1/N_1 - 1\right) - 1/\left(N-k\right)\right)} \tag{7}$$

where N is the total sample size and k is the number of groups and N_i is the sample size of the ith group and s_i^2 is the pooled variance.

Eq. (8) Levene's Test, which results in a F distribution of $(k-1, N-k)$ degrees of freedom (NIST/SEMATECH, 2005).

$$W = \frac{\left(N-k\right)\sum_{i=1}^{k} N_i \left(\hat{Z}_{i.} - \hat{Z}_{..}\right)^2}{\left(k-1\right)\sum_{i=1}^{k}\sum_{i=1}^{N_i} \left(Z_{ij} - \hat{Z}_{i.}\right)^2} \tag{8}$$

where N_i is the sample size of the ith group and k is the number of groups and $\hat{Z}_{i.}$ are the group means of Z_{ij} and $\hat{Z}_{..}$ is the overall mean of the Z_{ij} and $Z_{ij} = |Y_{ij} - \tilde{Y}_{i.}|$ and $\tilde{Y}_{i.}$ is the median of ith group.

The main difference between Bartlett's and Levene's test is their respective robustness to non-normality and to outliers. Levene's test, emphasizing the absolute difference from either the median or trimmed mean should theoretically be less susceptible to outliers. The question of which of these tests to use for MACACC analysis will be addressed in the section on applications to normal development.

Multiple comparisons

In MACACC, as for any statistical technique in brain-imaging, the error rate due to multiple comparisons has to be controlled for. Depending on the exact test used, MACACC produces P values generated from t, F, or $\times^2$ distribution. The resulting values can be corrected using standard techniques, such as Bonferroni correction, Random Field Theory (Worsley et al., 1992, 1996, 1999, 2004), Permutation testing (Nichols and Holmes, 2002; Nichols and Hayasaka, 2003), or the False Discovery Rate (FDR) (Genovese et al., 2002). We used FDR since it provides the greatest ability to threshold data stemming from multiple different statistical tests simultaneously, as described in (Lerch et al., 2005). The interpretation by FDR theory is thus that, of all the vertices shown as significant at the 0.05 level in this paper, 5% will be false positives.

Table 2
Population characteristics

	N	Age	IQ
Male	157	11.1 ± 3.8	116.4 ± 12.7
Female	135	12.0 ± 3.9	112.5 ± 13.4

Using residuals

MACACC analyses performed on raw cortical thickness data can be dominated by main effects occurring within the population being studied, most obviously age-related changes (Thompson et al., 2000; Giedd, 2004; Gogtay et al., 2004). To remove this confound a linear regression of age was first performed at every vertex, and the residuals of that regression substituted for the raw cortical thickness values. Similar procedures removed gender differences.

Application to normal development

The methods described above will be illustrated in a normal development population. The sample consists of 292 adolescents, characterized in Table 2.

MR Images were acquired on a 1.5-T General Electric Signa scanner (Milwaukee, Wis). T1-weighted images with contiguous 1.5-mm slices in the axial plane and 2.0-mm slices in the coronal plane were obtained using 3-dimensional spoiled gradient recalled echo in the steady state. Imaging parameters were echo time of 5 ms, repetition time of 24 ms, flip angle of 45°, acquisition matrix of 256 × 192, number of excitations equals 1, and 24 cm field of view. All subjects were tested using age appropriate versions of the Weschler intelligence scales (the WPPSI-III for children 4 to 6; the WISC-III or WASI for 6 to 17 years and the WAIS-III for 18 and above (Wechsler, 1991)) (Table 3).

Correlation strength

MACACC-strength measures the degree to which any part of the cortex correlates with the rest of the cortex. If one assumes that areas of the cortex with related function should correlate with each other to a greater degree, then one can expect that those areas of the cortex which relate to the greatest number of cortical regions will feature the highest MACACC-strength: the association cortices. These serve an integrative function, receiving inputs from multiple cortical and non-cortical sources, and in turn distributing information to multiple areas. The results of MACACC-strength in the entire population sample are shown in Fig. 3. As expected, the highest MACACC-strength was found in the association cortices, the lowest in the primary motor, sensorimotor, and visual areas.

Seed region: BA 44

As an example of the use of MACACC to assess a specific cortical area's correlation with other cortical areas, we used left Brodmann Area 44 (BA 44). We used a probability map derived from cytoarchitectonic data and non-linearly transformed into stereotaxic space for our regional definition (Amunts et al., 1999), as shown in Fig. 4a. BA 44 is part of Broca's area and primarily implicated in high-level aspects of speech production (Klein et al., 1995, 1997; Amunts et al., 2004; Fiebach et al., 2005), as well as potentially involved in imitation (Heiser et al., 2003; Makuuchi, 2005) and music perception (Platel et al., 1997). It is connected through the arcuate and uncinate fasciculi to other language areas, including Wernicke's and BA 40 (Petrides and Pandya, 1988; Chertkow and Murtha, 1997; Duffau et al., 2002; Parker et al., 2005).

We first used a BA 44 seed region to map the MACACC of BA 44 in the entire population sample, followed by an investigation of age differences for this map. Given its involvement in the language circuit, one would expect BA 44 to correlate strongly with functionally related areas such as Wernicke's area, the superior temporal gyrus, and BA 40 and 39. The results of this analysis are shown in Fig. 4b. The cortical thickness of BA 44 correlates with neighboring frontal regions, the large extent of these correlations is possibly due to the expansive definition of BA 44 used in this study. The MACACC map outside of the frontal lobes shows a striking similarity to tractographic maps of the arcuate fasciculus (Parker et al., 2005), encompassing inferior parietal areas along with the lateral temporal lobes and containing much of the language network. These correlations were highly significant, exceeding a correlation coefficient of 0.8.

Developmental MACACC differences

The cerebral cortex undergoes profound change throughout normal childhood development, particularly through the reorganization of synaptic and axonal contacts. Synaptic pruning is especially relevant for our dataset, as it is a continuous process from ages two to sixteen (Rivkin, 2000). The thickness of the cortex declines throughout most of the cerebrum with the exception of the temporal poles where continuous growth can be observed (Sowell et al., 2004).

Given the degree of structural change observed throughout development and the coincident maturation of language abilities, one can hypothesize age-related MACACC changes within our sample. Recent diffusion tensor imaging work has shown that the arcuate fasciculus changes in fractional anisotropy during normal development within an age range similar to that of our sample (Schmithorst et al., 2002).

Furthermore, fMRI has shown that lateralization of language function increases, and that BA 44 BOLD activity correlates with

Table 3
Age groupings: demographics of the three different age groups used to explore developmental MACACC differences

	Young		Middle		Old	
	N	Mean Age ± SD	N	Mean Age ± SD	N	Mean Age ± SD
Male	45	6.7 ± 1.4	77	11.5 ± 1.5	35	16.3 ± 1.8
Female	28	6.9 ± 1.5	70	11.4 ± 1.6	37	16.9 ± 2.2

Gender distribution is well balanced in the middle and old age group, though dominantly male in the youngest age grouping. This imbalance is negated by the fact that the MACACC analysis is performed on the residuals of a regression removing the main effect of age (see Using residuals).

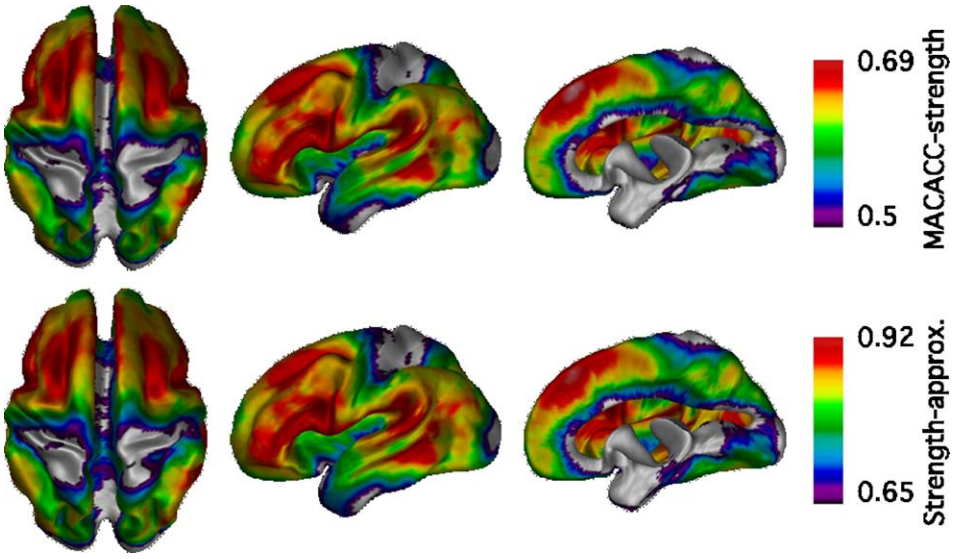

Fig. 3. MACACC-strength: Three view of the correlation strength of the entire population sample (n = 292) are shown in the top part of the figure. The association cortices clearly have the highest strength, primary motor, sensorimotor, and visual cortices the least. The exception here are the temporal poles, which feature surprisingly low MACACC-strength, possibly due to the assumption of linearity when removing age dependent effects. The bottom figure shows the MACACC-strength approximation, computed by correlating every vertex against mean cortical thickness. The results clearly look similar, albeit at different thresholds, and took 30 s to compute, as compared to the three days for the correct measure of MACACC-strength.

age (Holland et al., 2001). To test for MACACC age-related differences we subdivided our population into age-specific groupings, the young group containing subjects of less than 8.8 years, the old group older than 14.2 years, the middle group in between. The groupings were obtained by subdividing the entire population's age range into four groups of equal numbers of subjects, and combining the middle two groups in order to retain a simpler statistical model. Age was controlled for within each of the groupings. Both MACACC-slope and MACACC-variance were analyzed and the results are show in Fig. 5. Significant differences were observed between the older and younger subjects. The slope relating BA 44 and the bilateral superior temporal gyri (STG) is steeper in older subjects. Moreover, the variance differs in the STG, the medial frontal lobes, right Broca's Area, right orbito-frontal cortex, and bilateral lateral parietal lobes. In all cases the variance is less in the older subjects. These maps thus indicate an increasing correlation with age between the left BA 44 and its counterparts in the language network and frontal lobe circuits.

Variance tests

As discussed in the methods section, multiple tests for group differences in variance were assessed. The results of different variance tests are shown in Fig. 6; the overall patterns are clearly similar. Robustness to outliers, however, is where the tests differed most. Fig. 6 shows that a single outlier can have tremendous influence on the estimation of variance, and that Levene's Test is the most robust to this outlier. For that reason Levene's Test was chosen for testing MACACC-variance.

IQ MACACC differences

General measures of intelligence correlate with global grey matter volumes (Andreasen et al., 1993; Reiss et al., 1996; Pennington et al., 2000; Posthuma et al., 2003; Wilke et al., 2003; Haier et al., 2004). Correlations with particular cortical areas are, however, limited. This leads to the hypothesis that IQ is a property of the cortex better understood in terms of interactions

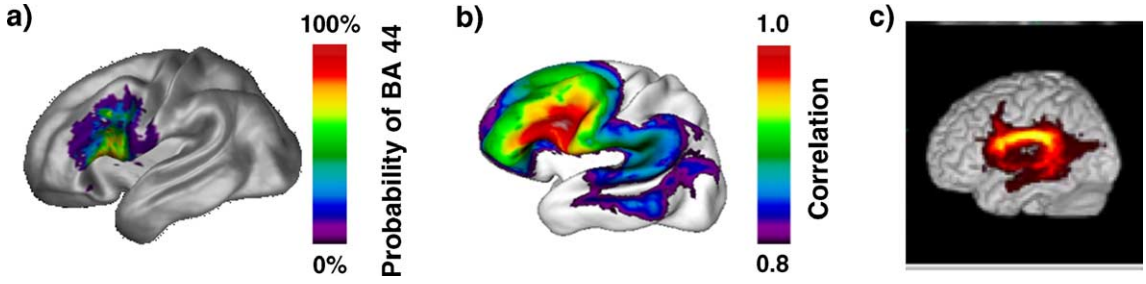

Fig. 4. MACACC of BA 44. Part a shows the probability map of Brodmann Area 44 used as the seed region, obtained from (Amunts et al., 1999). Part b shows the MACACC map generated from the 292 subjects, i.e., every vertex across the entire population is correlated with the mean thickness of the seed region shown in part a. Part c, reproduced from (Parker et al., 2005), shows the diffusion tensor imaging probability map of Broca's area connections through the arcuate and uncinate fasciculi. The correlation map features strong correlations throughout the frontal lobes, possibly due to the expansive BA 44 probability map used, but the extra-frontal lobe correlations show a pattern remarkably similar to the tractography of the arcuate fasciculus.

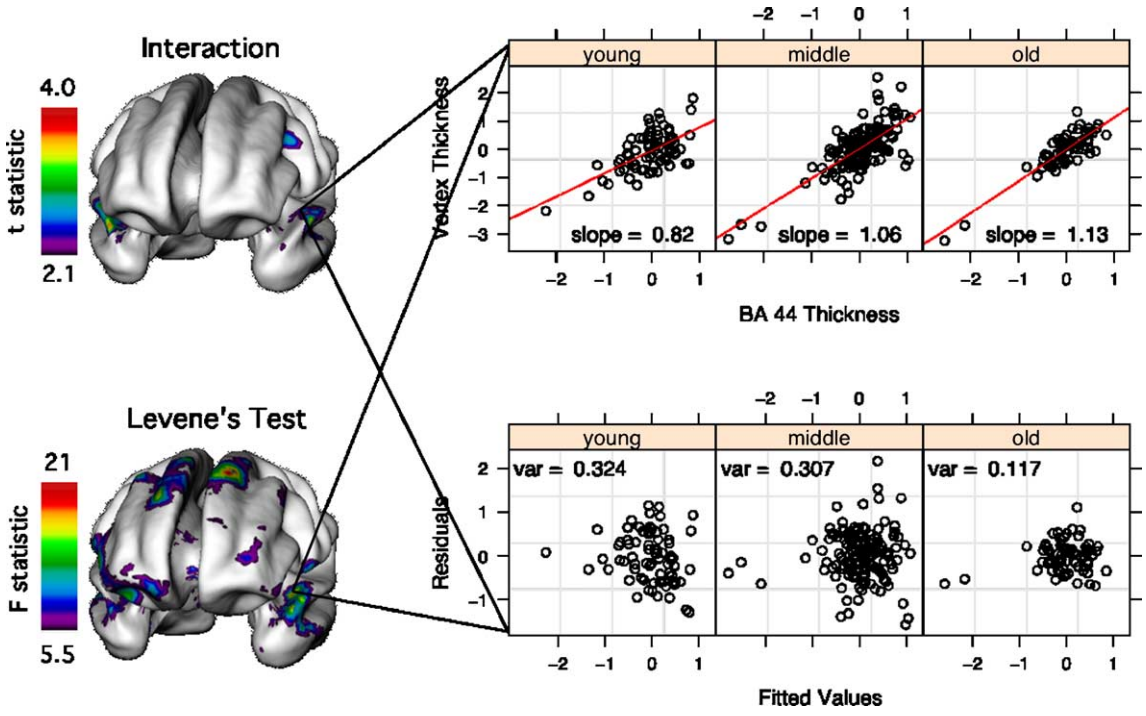

Fig. 5. MACACC age difference. Significant age by BA 44 interactions can be found in the bilateral STG, though the main effect appears to be in the differences in variance between the groups, where the bilateral STG are significant as well as multiple frontal and lateral temporal lobe areas. The plot shows one vertex in the left STG, describing both the slopes (top) as well as variance in a plot of residuals against fitted values (bottom) for each of the three age groups (young, middle, old; see text). Levene's test was the only variance test employed as it proved the most robust (see Fig. 6).

between different cerebral regions (Wilke et al., 2003). We tested this hypothesis by dividing our population into low (<100) and high (>120) IQ sub-samples and testing for MACACC-slope and MACACC-variance differences with left BA 44 as the seed region. The results are shown in Fig. 7. The principal differences were found in the MACACC-slope analysis in the ventro- and dorsolateral prefrontal cortex, the lateral parietal lobes, and the anterior cingulate. The focus on the cingulate confirms previous IQ morphometry studies (Wilke et al., 2003), and extends them by showing a network of regions differentiating low and high IQ

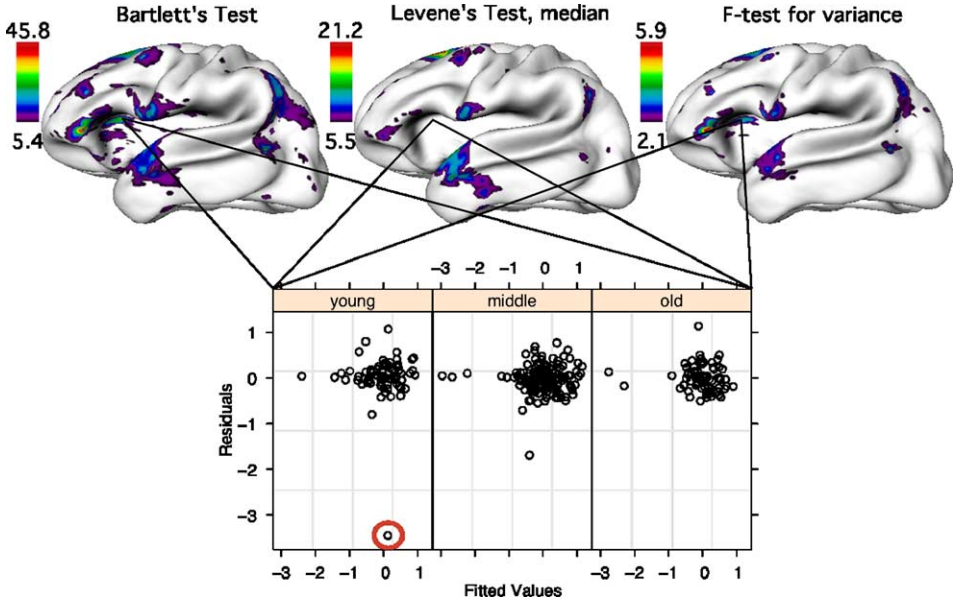

Fig. 6. MACACC-variance tests: the differences in variance as estimated using three statistical tests are shown, revealing similar patterns of significance. One difference, however, can be found in the left insula, and a plot of the residuals for all 292 subjects at this vertex shows that a single outlier (circled in red, and likely a methodological error) is driving significance in the *F* test for variance and Bartlett's test. Levene's test, on the other hand, is robust against the influence of this outlier. In order to comply with the *F* test for variance's requirement of two groups all statistics compare the young versus old group only.

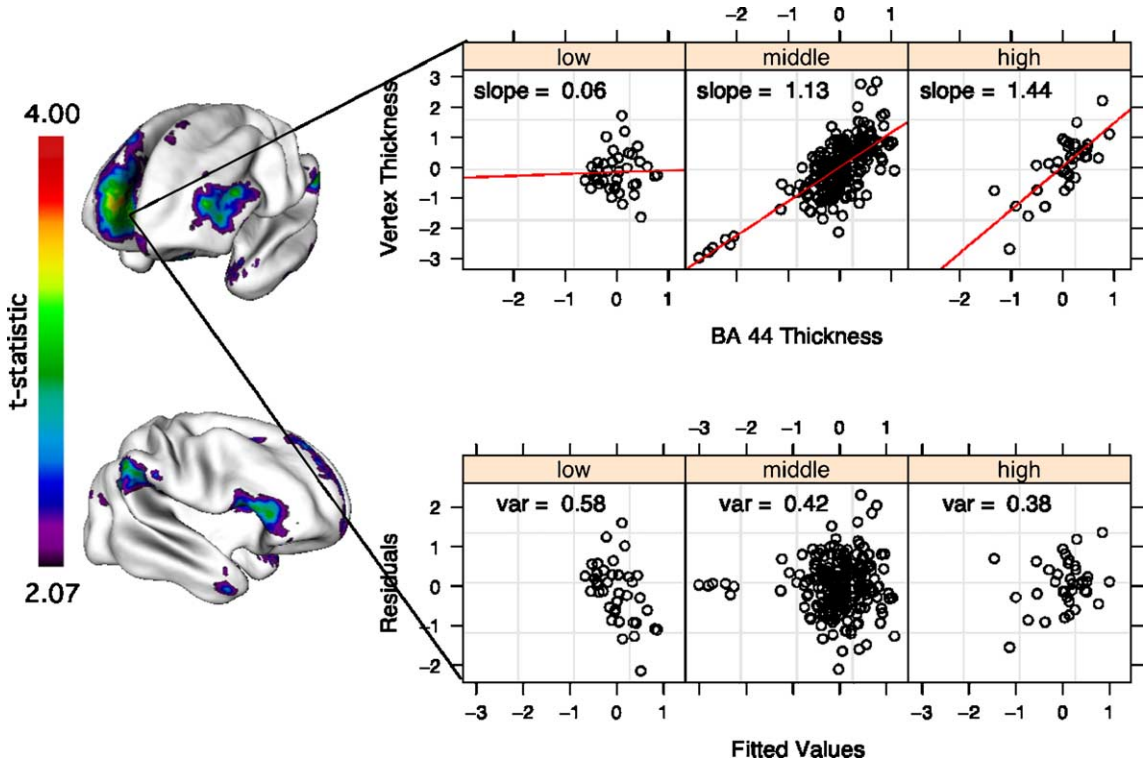

Fig. 7. IQ differences: this figure shows the MACACC differences between low and high IQ grouping in the population. There are significant MACACC-slope differences in the ventro and dorsolateral prefrontal cortex, the lateral parietal lobes, and, most significantly, the right anterior cingulate. The graph shows the BA 44 to cingulate slope (top) and variance (bottom) differences. Note the difference in slopes between the IQ groups. MACACC-variance tests (not shown) were insignificant except for one small peak in the right superior temporal gyrus.

subjects involving prefrontal, lateral parietal, and anterior temporal lobes.

Discussion

We have introduced a new strategy for analyzing correlated changes in cortical morphology within a population sample. The MACACC methods can be used to study the correlated connectivity of a seed region, to assess the total correlation strength at every point in the cortex, and to investigate differences in cross-cortical correlations between subject groupings. We chose the correlations approach as it was found to have greater regional specificity than related techniques such as singular value decomposition (Worsley et al., 2005). MACACC-strength tests, which reveal the relative inter-connectivity of every vertex, require no prior hypotheses, and can thus be used to assess global population differences. MACACC-slope and MACACC-variance tests, on the other hand, are designed to be used with a seed region, and thus require a prior hypothesis. Given a seed region, precise investigations of group differences within a cortical network involving the seed region can then be obtained and tested for significance.

The results from the normal brain development population are intriguing and encouraging. While MACACC maps are not the same as anatomical connectivity measured with fibre tracking, the correlation maps of BA 44 do bear a striking resemblance to the diffusion tensor maps of the arcuate fasciculus (Fig. 4), suggesting that they are measuring parts of the same underlying processes. In the population studied, different cortical areas within the language network correlated tightly; we thus predict that future MACACC studies will show similar structural relationships in different cortical networks.

The MACACC map of BA 44 showed an age-related tightening of the correlation with the superior temporal gyrus (Fig. 5), which is connected to BA 44 through the arcuate and uncinate fasciculi (Parker et al., 2005). The STG, like BA 44, is involved in the anatomical network underlying language (Dronkers et al., 2004; Matsumoto et al., 2004; Parker et al., 2005) and auditory function (Platel et al., 1997; Romanski et al., 1999; Kiehl et al., 2001; Jeffries et al., 2003; Kim et al., 2004). The tightening of correlations is occurring concurrently with expanding language function within the age range studied (Holland et al., 2001; Schmithorst et al., 2002). This suggests that MACACC is capturing an important part of the normal brain development process, wherein the thickness of the cortex between areas subserving related functional specializations show greater similarity to each other with age, while simultaneously white matter tracts connecting these areas mature (Paus et al., 1999, 2001; Schmithorst et al., 2002), a pattern likely to be especially prevelant in the frontal lobes, since they are the last to fully myelinate in the cerebrum (Schneider et al., 2004). Abnormal development would thus be suspected of showing different correlation patterns or an absence of this tightening effect of the correlation maps.

We furthermore report stepwise increases in connectivity between BA 44, the ACC and parietal cortex linked to increasing intellectually ability, reflected by IQ (Fig. 7). Meta-analyses of fMRI studies have implicated the inferior frontal gyrus as a core region in supporting diverse cognitive tasks which supports our use of BA 44 as a ‘seed’ region (Duncan et al., 2000). The

strengthened pattern of correlations between this hub and fronto-parietal regions bear a striking resemblance to the functional activation network shown by Gray to vary with intelligence (Gray et al., 2003). We identify the ACC and parietal cortex as structural correlates of the lateral frontal cortex regions which have been implicated in the allocation of attentional resources, planning and cognitive control, all core facets of intelligence (Andreasen et al., 1993; Reiss et al., 1996; Rubia et al., 2000; Paus, 2001; Booth et al., 2003; Wilke et al., 2003; Haier et al., 2004; Toga and Thompson, 2004). Future studies should investigate MACACC differences using IQ subtests or other psychometric measures providing indices of more isolated functional paradigms.

What is particularly interesting is that the type of group differences in the IQ and age studies varies: the main results for age differences shows a change in MACACC-variance, as the correlations tighten with age. With IQ, on the other hand, the key findings are in MACACC-slope, as the type of correlation with the seed region is different in the high and low IQ groups. The tightening correlations with age capture an ongoing developmental process. Different slopes in the IQ case suggest that the cortical areas implicated interact in a differently coupled fashion. The relationship between BA 44 and the anterior cingulate graphed in Fig. 7 indicates that, in the low IQ group, the thickness of the cingulate barely increases with an increase in the cortical thickness of BA 44. In the high IQ group, on the other hand, an increase of 1 mm in BA 44 predicts an increase of 1.44 mm in the cingulate. The fact that such different relationships can exist within the same population divided by IQ suggests that the biological underpinnings of such changes should be further investigated.

The biological causes underlying correlations between the cortical thickness of related brain areas are not well defined. The idea that behavioral modifications can induce plastic changes in the cerebrum is not new; as early as 1904 Santiago Ramon y Cajal hypothesized that skill acquisition must require the strengthening of existing and formation of new pathways (Pascual-Leone et al., 2005). Multiple studies have hinted at changes in cortico-cortico or cortico-sub-cortical coherence in response to alternations in afferent input or efferent demand. These changes are likely accompanied by the formations of new connections through dendritic growth and arborization (Pascual-Leone et al., 2005). Such modifications of the neuropil will feature changes in the thickness of the cortex. Combined with the normal patterns of cortical development occurring within the age range studied herein, these processes are the likely driving forces behind MACACC. Such statements can at this point in time only be speculative, however, and need to be further investigated.

Based on the above discussion, we predict that degenerative disorders such as Alzheimer's Disease will show increasing dissociation between related areas, resulting in significant MACACC-variance differences. Disorders such as schizophrenia, hypothesized to be a connectivity disorder (Pearlson, 1999; Penn, 2001; Innocenti et al., 2003; de Haan and Bakker, 2004), would likely feature both MACACC-slope and variance differences.

The metric of choice for the study of MACACC was cortical thickness, which provides a biologically meaningful measure of cortical anatomy. Being derived from MR data in a complex series of image processing steps means, however, that cortical thickness as measured in this study is an approximation of the underlying anatomy, and therefore subject to several open questions. For example, the pre-central gyrus is relatively thin in our results, yet post-mortem studies suggest that it should be thicker (von Economo and Koskinas, 1925). The key limitation is likely the classification of cortical tissue into grey and white matter; in areas of the cortex where this can be reliably achieved the resulting cortical thickness measurements are likely accurate, in regions where this is more difficult, such as the heavily myelinated pre-motor cortex, the results might differ from histological examination.

Studying MACACC opens a new field of study to the imaging neurosciences. It is conceivable that certain anatomical patterns cannot be detected by simple models which relate morphometry to group or morphometry to cognitive/clinical variable, but instead lie in the relationship between regions of the cortex. To give an example, Alzheimer's Disease involves characteristic thinning of the cortex (Gomez-Isla et al., 1997; Lerch et al., 2005). What is less certain is how early into the disease progression cortical thinning becomes detectable, especially given the noise inherent in an in vivo imaging study. A potentially more sensitive indicator of onset of the AD pathological processes is the statistical relationship between the morphometry of limbic system structures known to be involved in the early stages of the disease (Braak and Braak, 1991; Delacourte et al., 1999).

The MACACC methods described here still need to be extended and further explored. The most important addition will be to extend MACACC to longitudinal and mixed models, where one can look for changes in correlation not just across populations but within single subjects. Further work also needs to include better handling of continuous data for MACACC-variance tests. Methods such as Levene's and Bartlett's test need discrete groupings. One potential solution is to use general least squares with a weights structure reflecting change in variance with the continuous variable, and perform a likelihood ratio test to ascertain whether allowing for non-uniform error improves the model fit.

To conclude, we propose that studying MACACC opens a new field of study to the imaging neurosciences, providing a structural methodology for delineating cortical correlations which complements current techniques defining anatomical and functional connectivity.

Acknowledgments

ICBM grant PO1MHO52176-11, principal investigator Dr. John Mazziotta; CIHR grant MOP-34996. Jason Lerch is funded by a K.M. Hunter/CIHR Doctoral Research Award. We thank Dr. Alex Zijdenbos for his many insightful comments on this work.

References

Amunts, K., Schleicher, A., Burgel, U., Mohlberg, H., Uylings, H.B., Zilles, K., 1999. Broca's region revisited: cytoarchitecture and intersubject variability. J. Comp. Neurol. 412 (2), 319–341.

Amunts, K., Weiss, P.H., Mohlberg, H., Pieperhoff, P., Eickhoff, S., Gurd, J.M., et al., 2004. Analysis of neural mechanisms underlying verbal fluency in cytoarchitectonically defined stereotaxic space—The roles of Brodmann areas 44 and 45. NeuroImage 22 (1), 42–56.

Andreasen, N.C., Flaum, M., Swayze, V.N., O'Leary, D.S., Alliger, R., Cohen, G., et al., 1993. Intelligence and brain structure in normal individuals. Am. J. Psychiatry 150 (1), 130–134.

Ashburner, J., Friston, K.J., 2000. Voxel-based morphometry—The methods. NeuroImage 11 (6 Pt. 1), 805–821.

Booth, J.R., Burman, D.D., Meyer, J.R., Lei, Z., Trommer, B.L., Davenport, N.D., et al., 2003. Neural development of selective attention and response inhibition. NeuroImage 20 (2), 737–751.

Braak, H., Braak, E., 1991. Neuropathological stageing of Alzheimer-related changes. Acta Neuropathol. (Berl.) 82 (4), 239–259.

Buckner, R.L., Raichle, M.E., Petersen, S.E., 1995. Dissociation of human prefrontal cortical areas across different speech production tasks and gender groups. J. Neurophysiol. 74 (5), 2163–2173.

Chertkow, H., Murtha, S., 1997. PET activation and language. Clin. Neurosci. 4 (2), 78–86.

Chung, M.K., Worsley, K.J., Robbins, S., Paus, T., Taylor, J., Giedd, J.N., et al., 2003. Deformation-based surface morphometry applied to gray matter deformation. NeuroImage 18 (2), 198–213.

Collins, D.L., Neelin, P., Peters, T.M., Evans, A.C., 1994. Automatic 3D intersubject registration of MR volumetric data in standardized Talairach space. J. Comput. Assist. Tomogr. 18 (2), 192–205.

de Haan, L., Bakker, J.M., 2004. Overview of neuropathological theories of schizophrenia: from degeneration to progressive developmental disorder. Psychopathology 37 (1), 1–7.

Delacourte, A., David, J.P., Sergeant, N., Buee, L., Wattez, A., Vermersch, P., et al., 1999. The biochemical pathway of neurofibrillary degeneration in aging and Alzheimer's disease. Neurology 52 (6), 1158–1165.

Dronkers, N.F., Wilkins, D.P., Van Valin, R.D.J., Redfern, B.B., Jaeger, J.J., 2004. Lesion analysis of the brain areas involved in language comprehension. Cognition 92 (1–2), 145–177.

Duffau, H., Capelle, L., Sichez, N., Denvil, D., Lopes, M., Sichez, J.P., et al., 2002. Intraoperative mapping of the subcortical language pathways using direct stimulations. An anatomo-functional study. Brain 125 (Pt. 1), 199–214.

Duncan, J., Seitz, R.J., Kolodny, J., Bor, D., Herzog, H., Ahmed, A., et al., 2000. A neural basis for general intelligence. Science 289 (5478), 457–460.

Fiebach, C.J., Schlesewsky, M., Lohmann, G., von Cramon, D.Y., Friederici, A.D., 2005. Revisiting the role of Broca's area in sentence processing: syntactic integration versus syntactic working memory. Hum. Brain Mapp. 24 (2), 79–91.

Friedman, L., Kenny, J.T., Wise, A.L., Wu, D., Stuve, T.A., Miller, D.A., et al., 1998. Brain activation during silent word generation evaluated with functional MRI. Brain Lang. 64 (2), 231–256.

Friston, K., 2002. Beyond phrenology: what can neuroimaging tell us about distributed circuitry? Annu. Rev. Neurosci. 25, 221–250.

Friston, K.J., Frith, C.D., Liddle, P.F., Frackowiak, R.S., 1993. Functional connectivity: the principal-component analysis of large (PET) data sets. J. Cereb. Blood Flow Metab. 13 (1), 5–14.

Friston, K.J., Frith, C.D., Fletcher, P., Liddle, P.F., Frackowiak, R.S., 1996. Functional topography: multidimensional scaling and functional connectivity in the brain. Cereb. Cortex 6 (2), 156–164.

Friston, K.J., Harrison, L., Penny, W., 2003. Dynamic causal modelling. NeuroImage 19 (4), 1273–1302.

Frith, C.D., Friston, K.J., Liddle, P.F., Frackowiak, R.S., 1991. A PET study of word finding. Neuropsychologia 29 (12), 1137–1148.

Gaser, C., Schlaug, G., 2003a. Gray matter differences between musicians and nonmusicians. Ann. N. Y. Acad. Sci. 999, 514–517.

Gaser, C., Schlaug, G., 2003b. Brain structures differ between musicians and non-musicians. J. Neurosci. 23 (27), 9240–9245.

Genovese, C.R., Lazar, N.A., Nichols, T., 2002. Thresholding of statistical maps in functional neuroimaging using the false discovery rate. NeuroImage 15 (4), 870–878.

Giedd, J.N., 2004. Structural magnetic resonance imaging of the adolescent brain. Ann. N. Y. Acad. Sci. 1021, 77–85.

Gogtay, N., Giedd, J.N., Lusk, L., Hayashi, K.M., Greenstein, D., Vaituzis, A.C., et al., 2004. Dynamic mapping of human cortical development during childhood through early adulthood. Proc. Natl. Acad. Sci. U. S. A. 101 (21), 8174–8179.

Golestani, N., Paus, T., Zatorre, R.J., 2002. Anatomical correlates of learning novel speech sounds. Neuron 35 (5), 997–1010.

Gomez-Isla, T., Hollister, R., West, H., Mui, S., Growdon, J.H., Petersen, R.C., et al., 1997. Neuronal loss correlates with but exceeds neurofibrillary tangles in Alzheimer's disease. Ann. Neurol. 41 (1), 17–24.

Gray, J.R., Chabris, C.F., Braver, T.S., 2003. Neural mechanisms of general fluid intelligence. Nat. Neurosci. 6 (3), 316–322.

Haier, R.J., Jung, R.E., Yeo, R.A., Head, K., Alkire, M.T., 2004. Structural brain variation and general intelligence. NeuroImage 23 (1), 425–433.

Heiser, M., Iacoboni, M., Maeda, F., Marcus, J., Mazziotta, J.C., 2003. The essential role of Broca's area in imitation. Eur. J. Neurosci. 17 (5), 1123–1128.

Holland, S.K., Plante, E., Weber Byars, A., Strawsburg, R.H., Schmithorst, V.J., Ball, W.S.J., 2001. Normal fMRI brain activation patterns in children performing a verb generation task. NeuroImage 14 (4), 837–843.

Horwitz, B., 2003. The elusive concept of brain connectivity. NeuroImage 19 (2 Pt. 1), 466–470.

Innocenti, G.M., Ansermet, F., Parnas, J., 2003. Schizophrenia, neurodevelopment and corpus callosum. Mol. Psychiatry 8 (3), 261–274.

Jeffries, K.J., Fritz, J.B., Braun, A.R., 2003. Words in melody: an H(2)15O PET study of brain activation during singing and speaking. NeuroReport 14 (5), 749–754.

Kabani, N., Le Goualher, G., MacDonald, D., Evans, A.C., 2001. Measurement of cortical thickness using an automated 3-D algorithm: a validation study. NeuroImage 13 (2), 375–380.

Kiehl, K.A., Laurens, K.R., Duty, T.L., Forster, B.B., Liddle, P.F., 2001. Neural sources involved in auditory target detection and novelty processing: an event-related fMRI study. Psychophysiology 38 (1), 133–142.

Kim, D.E., Shin, M.J., Lee, K.M., Chu, K., Woo, S.H., Kim, Y.R., et al., 2004. Musical training-induced functional reorganization of the adult brain: functional magnetic resonance imaging and transcranial magnetic stimulation study on amateur string players. Hum. Brain Mapp. 23 (4), 188–199.

Kim, J.S., Singh, V., Lee, J.K., Lerch, J., Ad-Dab'bagh, Y., MacDonald, D., et al., 2005. Automated 3-D extraction and evaluation of the inner and outer cortical surfaces using a Laplacian map and partial volume effect classification. NeuroImage 27 (1), 210–221.

Klein, D., Milner, B., Zatorre, R.J., Meyer, E., Evans, A.C., 1995. The neural substrates underlying word generation: a bilingual functional-imaging study. Proc. Natl. Acad. Sci. U. S. A. 92 (7), 2899–2903.

Klein, D., Olivier, A., Milner, B., Zatorre, R.J., Johnsrude, I., Meyer, E., et al., 1997. Obligatory role of the LIFG in synonym generation: evidence from PET and cortical stimulation. NeuroReport 8 (15), 3275–3279.

Koski, L., Paus, T., 2000. Functional connectivity of the anterior cingulate cortex within the human frontal lobe: a brain-mapping meta-analysis. Exp. Brain Res. 133 (1), 55–65.

Lee, L., Harrison, L.M., Mechelli, A., 2003. A report of the functional connectivity workshop, Dusseldorf 2002. NeuroImage 19 (2 Pt. 1), 457–465.

Lerch, J.P., Evans, A.C., 2005. Cortical thickness analysis examined through power analysis and a population simulation. NeuroImage 24 (1), 163–173.

Lerch, J.P., Pruessner, J.C., Zijdenbos, A., Hampel, H., Teipel, S.J., Evans, A.C., 2005. Focal decline of cortical thickness in Alzheimer's disease identified by computational neuroanatomy. Cereb. Cortex 15 (7), 995–1001.

MacDonald, D., Kabani, N., Avis, D., Evans, A.C., 2000. Automated 3-D extraction of inner and outer surfaces of cerebral cortex from MRI. NeuroImage 12 (3), 340–356.

Maguire, E.A., Gadian, D.G., Johnsrude, I.S., Good, C.D., Ashburner, J., Frackowiak, R.S., et al., 2000. Navigation-related structural change in the hippocampi of taxi drivers. Proc. Natl. Acad. Sci. U. S. A. 97 (8), 4398–4403.

Maguire, E.A., Spiers, H.J., Good, C.D., Hartley, T., Frackowiak, R.S., Burgess, N., 2003. Navigation expertise and the human hippocampus: a structural brain imaging analysis. Hippocampus 13 (2), 250–259.

Makuuchi, M., 2005. Is Broca's area crucial for imitation? Cereb. Cortex 15 (5), 563–570.
Matsumoto, R., Nair, D.R., LaPresto, E., Najm, I., Bingaman, W., Shibasaki, H., et al., 2004. Functional connectivity in the human language system: a cortico-cortical evoked potential study. Brain 127 (Pt. 10), 2316–2330.
Nichols, T., Hayasaka, S., 2003. Controlling the familywise error rate in functional neuroimaging: a comparative review. Stat. Methods Med. Res. 12 (5), 419–446.
Nichols, T.E., Holmes, A.P., 2002. Nonparametric permutation tests for functional neuroimaging: a primer with examples. Hum. Brain Mapp. 15 (1), 1–25.
NIST/SEMATECH, 2005. e-Handbook of Statistical Methods. http://www.itl.nist.gov/div898/handbook/.
Parker, G.J., Luzzi, S., Alexander, D.C., Wheeler-Kingshott, C.A., Ciccarelli, O., Lambon Ralph, M.A., 2005. Lateralization of ventral and dorsal auditory–language pathways in the human brain. NeuroImage 24 (3), 656–666.
Pascual-Leone, A., Amedi, A., Fregni, F., Merabet, L.B., 2005. The plastic human brain cortex. Annu. Rev. Neurosci. 28, 377–401.
Paus, T., 2001. Primate anterior cingulate cortex: where motor control, drive and cognition interface. Nat. Rev., Neurosci. 2 (6), 417–424.
Paus, T., Zijdenbos, A., Worsley, K., Collins, D.L., Blumenthal, J., Giedd, J.N., et al., 1999. Structural maturation of neural pathways in children and adolescents: in vivo study. Science 283 (5409), 1908–1911.
Paus, T., Collins, D.L., Evans, A.C., Leonard, G., Pike, B., Zijdenbos, A., 2001. Maturation of white matter in the human brain: a review of magnetic resonance studies. Brain Res. Bull. 54 (3), 255–266.
Pearlson, G.D., 1999. New insights on the neuroanatomy of schizophrenia. Curr. Psychiatry Rep. 1 (1), 41–45.
Penn, A.A., 2001. Early brain wiring: activity-dependent processes. Schizophr. Bull. 27 (3), 337–347.
Pennington, B.F., Filipek, P.A., Lefly, D., Chhabildas, N., Kennedy, D.N., Simon, J.H., et al., 2000. A twin MRI study of size variations in human brain. J. Cogn. Neurosci. 12 (1), 223–232.
Petrides, M., Pandya, D.N., 1988. Association fiber pathways to the frontal cortex from the superior temporal region in the rhesus monkey. J. Comp. Neurol. 273 (1), 52–66.
Petrides, M., Pandya, D.N., 2002. Comparative cytoarchitectonic analysis of the human and the macaque ventrolateral prefrontal cortex and corticocortical connection patterns in the monkey. Eur. J. Neurosci. 16 (2), 291–310.
Pinheiro, J.C., Bates, D.M., 2000. Mixed-Effects Models in S and S-PLUS. Springer, New York.
Platel, H., Price, C., Baron, J.C., Wise, R., Lambert, J., Frackowiak, R.S., et al., 1997. The structural components of music perception. A functional anatomical study. Brain 120 (Pt. 2), 229–243.
Posthuma, D., Baare, W.F., Hulshoff Pol, H.E., Kahn, R.S., Boomsma, D.I., De Geus, E.J., 2003. Genetic correlations between brain volumes and the WAIS-III dimensions of verbal comprehension, working memory, perceptual organization, and processing speed. Twin Res. 6 (2), 131–139.
Ramnani, N., Behrens, T.E., Penny, W., Matthews, P.M., 2004. New approaches for exploring anatomical and functional connectivity in the human brain. Biol. Psychiatry 56 (9), 613–619.
Reiss, A.L., Abrams, M.T., Singer, H.S., Ross, J.L., Denckla, M.B., 1996. Brain development, gender and IQ in children. A volumetric imaging study. Brain 119 (Pt. 5), 1763–1774.
Rivkin, M.J., 2000. Developmental neuroimaging of children using magnetic resonance techniques. Ment. Retard. Dev. Disabil. Res. Rev. 6 (1), 68–80.
Robbins, S., Evans, A.C., Collins, D.L., Whitesides, S., 2004. Tuning and comparing spatial normalization methods. Med. Image Anal. 8 (3), 311–323.
Romanski, L.M., Bates, J.F., Goldman-Rakic, P.S., 1999. Auditory belt and parabelt projections to the prefrontal cortex in the rhesus monkey. J. Comp. Neurol. 403 (2), 141–157.
Rosas, H.D., Liu, A.K., Hersch, S., Glessner, M., Ferrante, R.J., Salat, D.H., et al., 2002. Regional and progressive thinning of the cortical ribbon in Huntington's disease. Neurology 58 (5), 695–701.
Rubia, K., Overmeyer, S., Taylor, E., Brammer, M., Williams, S.C., Simmons, A., et al., 2000. Functional frontalisation with age: mapping neurodevelopmental trajectories with fMRI. Neurosci. Biobehav. Rev. 24 (1), 13–19.
Salat, D.H., Buckner, R.L., Snyder, A.Z., Greve, D.N., Desikan, R.S., Busa, E., et al., 2004. Thinning of the cerebral cortex in aging. Cereb. Cortex 14 (7), 721–730.
Schlaug, G., 2001. The brain of musicians. A model for functional and structural adaptation. Ann. N. Y. Acad. Sci. 930, 281–299.
Schmithorst, V.J., Wilke, M., Dardzinski, B.J., Holland, S.K., 2002. Correlation of white matter diffusivity and anisotropy with age during childhood and adolescence: a cross-sectional diffusion-tensor MR imaging study. Radiology 222 (1), 212–218.
Schneider, J.F., Il'yasov, K.A., Hennig, J., Martin, E., 2004. Fast quantitative diffusion-tensor imaging of cerebral white matter from the neonatal period to adolescence. Neuroradiology 46 (4), 258–266.
Sled, J.G., Zijdenbos, A.P., Evans, A.C., 1998. A nonparametric method for automatic correction of intensity nonuniformity in MRI data. IEEE Trans. Med. Imaging 17 (1), 87–97.
Sowell, E.R., Thompson, P.M., Leonard, C.M., Welcome, S.E., Kan, E., Toga, A.W., 2004. Longitudinal mapping of cortical thickness and brain grown in normal children. Neuroscience 24 (38), 8223–8231.
Thompson, P.M., Giedd, J.N., Woods, R.P., MacDonald, D., Evans, A.C., Toga, A.W., 2000. Growth patterns in the developing brain detected by using continuum mechanical tensor maps. Nature 404 (6774), 190–193.
Toga, A.W., Thompson, P.M., 2004. Genetics of brain structure and intelligence. Annu. Rev. Neurosci.
von Economo, K., Koskinas, G., 1925. Die Cytoarchitektonik der Hirnrinde des erwachsenen Menschen. Julius Springer, Berlin.
Watkins, K.E., Paus, T., Lerch, J.P., Zijdenbos, A., Collins, D.L., Neelin, P., et al., 2001. Structural asymmetries in the human brain: a voxel-based statistical analysis of 142 MRI scans. Cereb. Cortex 11 (9), 868–877.
Wechsler, D. (1991). WISC-III: Wechsler intelligence scale for children: manual. San Antonio: Psychological Corp., Harcourt Brace Jovanovich.
Wilke, M., Sohn, J.H., Byars, A.W., Holland, S.K., 2003. Bright spots: correlations of gray matter volume with IQ in a normal pediatric population. NeuroImage 20 (1), 202–215.
Worsley, K.J., Evans, A.C., Marrett, S., Neelin, P., 1992. A three-dimensional statistical analysis for CBF activation studies in human brain. J. Cereb. Blood Flow Metab. 12 (6), 900–918.
Worsley, K.J., Marrett, S., Neelin, P., Vandal, A.C., Friston, K.J., Evanc, A.C., 1996. A unified statistical approach for determining significant signal in images of cerebral activation. Hum. Brain Mapp. 4, 58–73.
Worsley, K.J., Andermann, M., Koulis, T., MacDonald, D., Evans, A.C., 1999. Detecting changes in nonisotropic images. Hum. Brain Mapp. 8 (2–3), 98–101.
Worsley, K.J., Taylor, J.E., Tomaiuolo, F., Lerch, J., 2004. Unified univariate and multivariate random field theory. NeuroImage 23 (Suppl. 1), S189–S195.
Worsley, K.J., Chen, J.I., Lerch, J., Evans, A.C., 2005. Comparing functional connectivity via thresholding correlations and singular value decomposition. Philos. Trans. R. Soc. London, Ser. B Biol. Sci. 360 (1457), 913–920.
Zijdenbos, A.P., Forghani, R., Evans, A.C., 2002. Automatic "pipeline" analysis of 3-D MRI data for clinical trials: application to multiple sclerosis. IEEE Trans. Med. Imaging 21 (10), 1280–1291.